VOL. 13, NO. 6, MARCH 2018 ISSN 1819-6608
ARPN Journal of Engineering and Applied Sciences

www.arpnjournals.com

AN ANALYSIS OF FREQUENCY SELECTIVITY OF INDOOR POWER LINE CHANNELS FOR BROADBAND COMMUNICATION

Banty Tiru
Department of Physics, Gauhati University, Guwahati, Assam, India
E-Mail: banty_tiru@rediffmail.com

ABSTRACT

Power line communication uses the readily available power line for data communication. The power line channel is characterized by unpredictable noise, high attenuation and is highly frequency selective, making it a harsh medium for communication. Though the former two is not controllable, the latter is dependent on the network and may provide opportunities to minimize if not remove completely. In this paper, the frequency selectivity of various cables, loads and topologies are studied. The results show that, some cables and loads offer lesser frequency selective channels to communication signals than the other. An experimental verification of some test channels is also done. The results can be used in predicting the efficiency of the available power line when used as a communication medium and in the future design of cables and loads compatible for data transfer.

Keywords: power line communication, ABCD matrices, frequency selectivity, coherent bandwidth, RMS delay spread.

INTRODUCTION

Development of any communication system requires extensive study and modeling of the channel characteristics. This forms the basis of computer simulations aiming expectable performance. More so, for Power Line Communication (PLC) that uses power line (PL) as a communication medium independently or as components of a hybrid network. The reason is PLs suffer from unpredictable noise and channel characteristics and lack standard models that generalize the behavior. Though commented by some as 'horrible' [1] media for communication, the ubiquitous nature still motivates research to design systems that can compete with other options. The PLC can be used in wider applications like smart grid, control, access and in-house.

The main problem with PL channel is the frequency selectivity arising due to reflections at the myriad discontinuities constituting the network. Multipath reception with different propagation delays and phase cause fading in the signal leading to a non uniform transfer function (TF). The worst is when it encounters open or short circuited branches causing complete reflections of the incident wave. The notches also occur where the impedance of the loads in the branches is small. The number of notches increases with the length of the branches showing a periodic nature [2]. The attenuation is determined by the loads at the terminations and exaggerated by multiple ones at the same frequency. Frequency selectivity decreases the coherence bandwidth (CBW) thereby increasing the RMS Delay Spread (RMS-DS) and affecting the rate of data transmission. This is worsened in complex topologies having frequency dependent loads [3]. Various measures are being opted to deal with the frequency selectivity problem. One way is to use complex multicarrier technologies like Orthogonal Frequency Division Multiplexing (OFDMA) which are very suitable for such channels. Another way is studying the channel dependencies to decrease the notches or predict them so that suitable pre-coding schemes can be used to decrease the inter symbol interference. Recent PLC research has also aimed for simplifying the PL behaviors through standard channels, seeking determinism and analyzing channel statistically. It is remarked in [4] that, 'if properly modeled, the PL channel transfer function exhibits more determinism than commonly believed. This determinism should be exploited for robust modem design and system optimization'. Such studies have shown that there is an increase in CBW in a higher frequency band [5].

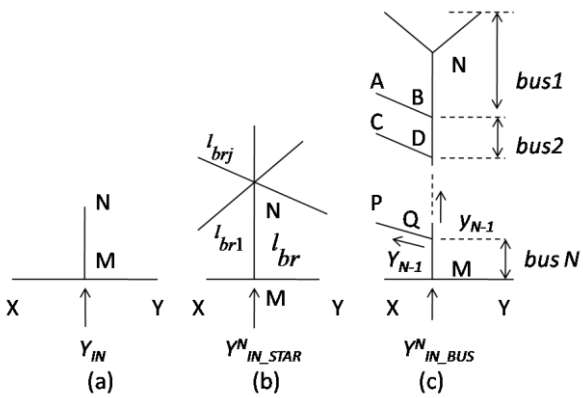

Figure-1. (a) Simple (b) star and (c) bus branch in PL channel.

Table-1. The cable parameters for different power line cables found in papers.

Cable	L µH/m	C pF/m	Z_0 Ω	LC 10^{-18}	R Ω/m	G S/m	Type	$\log_{10}$(LC)	Ref
(i)	0.69	38	135	26.22	1.94	1.08E-18	Type 2	-16.58	Present
(ii)	1.08	15	270	16.20	6.5E-3	0.58E-19	Type 1	-16.79	[6]
(iii)	0.96	17.5	234	16.80	5.1E-3	0.65E-19	Type 1	-16.77	[6]
(iv)	0.87	20	209	17.40	4.1E-3	0.72E-19	Type 1	-16.76	[6]
(v)	0.78	25	178	19.50	3.4E-3	0.80E-19	Type 1	-16.71	[6]
(vi)	0.68	33	143	22.44	2.7E-3	0.93E-19	Type 1	-16.65	[6]
(vii)	5.9	167	188	985.0	2.0E-6	6.14E-10	Type 1	-15.01	[7]
(viii)	4.6	130	188	598.0	2.3E-6	7.88E-10	Type 1	-15.22	[7]
(ix)	1.0	80	112	80.00	0.2	0.0003	Type 2	-16.10	[3]
(x)	0.041	156	16.2	6.4	0.32	0.0013	Type 2	-17.19	[8]
(xi)	0.6	120	70.7	72	0.4	0.0003	Type 2	-16.14	[3]
(xii)	0.083	313	16.33	25	0.4	0.0016	Type 2	-16.60	[9]
(xiii)	0.089	372	15.46	33	0.32	0.0013	Type 2	-16.48	[9]
(xiv)	0.262	133.94	52	48	1.98	0.0168	Type 2	-16.32	[10]
(xv)	0.65	40.3	127	26.19	0.400	0.0006	Type 2	-16.58	[11]

Moreover, PL channels are constituted of large variety of cable types, loads and topologies. Table-1 gives typical PL cables found in papers. The loads may also vary being frequency dependent or independent ones. The topology may be a simple or complex as *star* and *bus* branches as shown in Figure-1. A simple branch has only one branch (MN) in the propagation path (XY). A *star* branch has a large number of branches at a node (N) and a *bus* branch may have a large number emanating in a serial manner. The question therefore arises: How does the variability's affect the frequency selectivity of the channel? Can cables and loads be designed to decrease the selectivity suitably? How are the notches affected by complex topologies in the propagation path? In this paper, we deal with such questions, and aim to seek deterministic characteristics of the PL frequency selectivity. Such a study will aid in predicting the efficiency of PL cables and loads when used for communication and also in the future design of loads and cable that would serve the dual purpose of data and power transfer.

The paper is sectioned as follows: Section II of the paper gives an introduction to the PL channel modeling method and the basis of frequency selectivity. Section III studies the frequency selectivity and notches in the TF for different dependencies. Some simulated channels are also verified in experimental. Finally, in Section IV, a comparative study of communication parameters like CBW, Standard Deviation of CBW (σ) and RMS-DS are done for different cables and loads. The paper then concludes with the key results with possible applications of the same.

Power line channel modeling and notches

Modeling the PL channel is based on two methods: the time domain (top-down) and frequency domain (bottom-up) method. In the former; the parameters can be estimated only after the measurement of the actual TF and the computational cost of estimating the delay, phase and amplitude of each path are very high. The frequency domain approach is on the other hand simple to handle and uses the transmission line (TL) model (two or three wires, later termed as multi-conductor TL takes the ground conductor as well) to predict the TF accurately. The TL model assumes the signal to be propagated in a PL as Transverse Electromagnetic (TEM) wave and helps visualize the effect of all the reflections at the discontinuities enabling the salient features to be extracted. In this work, the second method is opted to use a two wire approach. The PL is considered as cascaded two port networks represented in terms of the ABCD or chain matrices. The ABCD matrices of the overall network can be written as the product of the matrices of the cascaded sections. The TF is written in terms of the overall ABCD matrices as

$$H(f) = \frac{Z_L}{AZ_L + B + CZ_S Z_L + DZ_S} \tag{1}$$

Where, Z_s and Z_L are source and load impedances respectively. The frequency selective notches, usually arises due to the branched tap, on the propagation path, the ABCD matrices of which are given by

$$ABCD_{Branched\_Tap} = \begin{bmatrix} 1 & 0 \\ 1/Z_{in} & 1 \end{bmatrix} \tag{2}$$

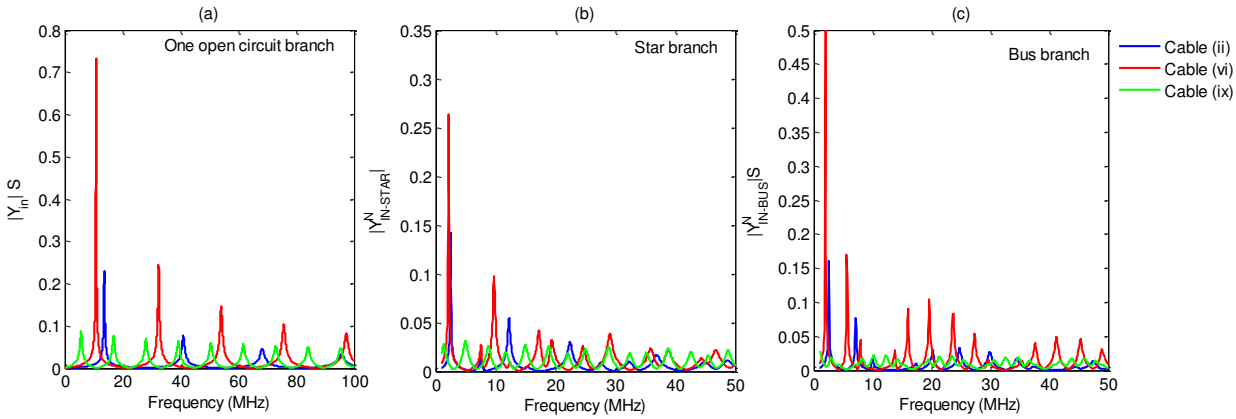

Figure-2. The magnitude of input admittance of different cables having (a) a simple open circuited branch (b) *star* topology with 3 number of branches at the node (c) *bus* topology with 3 number of buses.

$$Z_{in} = Z_0 \frac{Z_{br} + Z_0 \tanh(\gamma l_{br})}{Z_0 + Z_{br} \tanh(\gamma l_{br})} \tag{3}$$

Where Z_{in} is the input impedance of the branch loaded with load Z_{br} and γ is the propagation constant of the cable defined in terms of the primary line constants *R* (resistance/length), L (inductance/length), G (conductance/length) and C (capacitance/length) of the cable as given by (4)

$$\gamma = \sqrt{(R + jwL)(G + jwC)} = \alpha + j\beta \tag{4}$$

Here, *w* is the angular frequency and *α* and *β* are the phase and attenuation constants respectively. The notches are found in the frequencies where the input impedance is minimized. The input admittance (*IA*) of the branches is the inverse of Z_{in} and is maximum at the notch position.

$$Y_{in} = \frac{1}{Z_{in}} \tag{5}$$

Dependence of notches on channel variability

The notches depend on a large number of variables like types of cables, branch topology and load. In these sections, each variable is analyzed elaborately.

Cable parameters

The cable parameters *L* and *C* determine the open and short circuited notch due to a simple branch at frequencies (6) and (7) respectively.

$$f_{notch\_open} = \frac{2k+1}{4 l_{br} \sqrt{LC}} \tag{6}$$

$$f_{notch\_short} = \frac{k}{2 l_{br} \sqrt{LC}} \tag{7}$$

Here *k*=0, 1,……. As such, the difference between consecutive notches decreases with the increasing *LC* product of the cables. As seen in Table-1, the constant vary in a broad range from 6.4×10^{-18} to 985×10^{-18} and smaller values decrease the number of notches in the BW of observation. The *R* and *G* determine the attenuation of the notches. Figure-2(a) shows the plot of the *IA* characteristics of an open circuited branch (l_{br}=4.55m) for three different cables. The peaks in the *IA* determine the position of the notches in the TF. The cable such as *Cable (ii)* has smaller number of notches than *Cable (vi)* due to the small value of *LC*. On the other hand, *Cable (ix)* has a larger number of peaks with lesser heights. The reason is the larger value of *R/G*. The available cables can therefore be divided into two groups: *Type-1*: those having small *R* or/and *G* and *Type-2*: those having large *R* or/and *G*. *Type-1* cables are expected to yield channels having smaller CBW than *Type-2* cables.

Complex branches in the propagation path: star and bus topologies

For star topology branch as in Figure-1(b), the input admittance for N number of branches in the star node can be written as [12]

$$Y^N_{IN\_STAR} = \frac{1 + Z^N_{total} Y_{open}}{Z^N{}_{total} + Z_0^2 Y_{open}} \tag{8}$$

where Z^N_{total} is the total impedance offered by the *star* at the node N and Y_{open} is the *IA* of the branch if it were open (instead of having *star* branches). If all the branches in the *star* be open then the *IA* becomes

$$Y^N_{IN\_STAR} = \frac{1}{Z_0} \frac{1 + \dfrac{\tanh(\gamma l_{br})}{\sum_{j=1}^{N} \tanh(\gamma l_{brj})}}{\dfrac{1}{\sum_{j=1}^{N} \tanh(\gamma l_{brj})} + \tanh(\gamma l_{br})} \tag{9}$$

Where, $l_{brj}, j = 1,2...$ are the lengths of the branches in the star node, and l_{br} is the length of the branch to the node. The frequency of notches is therefore at positions where the denominator of (9) is the minimum which however cannot be determined accurately. However, it is in positions between the frequencies where the denominator is the maximum which can be accurately determined by (10).

$$(f)_{den\_max} = \frac{2k+1}{4l_{br1}\sqrt{LC}}, \frac{2k+1}{4l_{br2}\sqrt{LC}}, ..., \frac{k}{2l_{br}\sqrt{LC}}; k = 0,1.. \quad (10)$$

In general, for n numbers of f_{den_max}, the numbers of admittance maximum (n^{max}) is given by $n-1 < n^{max} < n+1$. Figure-2(a) shows the IA for 3 numbers of branches at the star node for different cables.

For bus configuration in the propagation path as in Figure-2(c), the IA for N number of bus connections can be written as

$$.Y^{N}_{IN\_BUS} = \frac{Y_{N-1} + y_{N-1} + Y_{open\_N-1}}{1 + Z_0^2 (Y_{N-1} + y_{N-1}) Y_{open\_N-1}} \quad (11)$$

Where Y_{N-1} and y_{N-1} are the IA of QP and QN at the node Q respectively and Y_{open_N-1} is the IA of MQ if it were open. In general,

$$y_i = \frac{Y_{i-1} + y_{i-1} + Y_{open\_i-1}}{1 + Z_0^2 (Y_{i-1} + y_{i-1}) Y_{open\_i-1}} \quad (12)$$

The elementary bus N=1 or bus 1 becomes a simple star branch with two branches at the nodes. The bus 1 and AB forms the load of bus 2. This continues till bus N is reached, the IA of which is $Y^{N}_{IN\_BUS}$ in the main path. The analysis becomes very complex when more numbers of sections are added. Figure-2(b) shows the IA for bus topology with 3 numbers of buses for different cables.

It is seen from Figure-2(b) and Figure-2(c) that cables such has Cable (ix) has a large number of peaks than Cable (ii) or Cable (vi) but the attenuation in the peaks is more due to larger R/G. Cable (vi) has a larger number of peaks than Cable (ii) due to smaller value of LC. As such, Type-1 cables are expected to yield lower CBW than Type-2 even in complex topologies. Type-1 cables with lower LC are also expected to yield larger CBW than those with larger LC.

Different types of loads in the branches

PL are loaded with loads that vary in wide ranges from frequency independent to frequency dependent ones [2], [13], [14]. The loads are categorized as (a) constant impedances (b) time invariant frequency dependent capacitive loads (c) time invariant frequency dependent inductive loads and (d) Constant complex loads (e) resonant circuits and (f) time variant loads. Some typical values referred in papers are ([5, 50, 135, 1000, 10^8] Ω, ([0.1, 1, 10, and 100] mH and ([$\in (0.1, 0.47)_{min,max}$] μF [2]. The resonant circuits can be modeled as parallel RLC circuits as [13]

$$Z(w) = \frac{R}{1 + jQ\left(\frac{w}{w_0} - \frac{w_0}{w}\right)} \quad (13)$$

consisting of R, the resistance at resonance, w_0, the resonant angular frequency ($w_0 = 2\pi f_0$) and Q, the quality factor. Typical values are given by $R \in \{200, 1800\}$, $f_0 \in \{2, 28\}$ MHz, and $Q \in \{5, 25\}$ [13]. The time variant loads are important only for low frequencies in <2MHz [15] and as such an analysis of the time invariant loads are done. To study the notch behavior for different load conditions, simulations are performed for a simple branch using *Cable (i)* in Table-1 having a characteristic impedance of Z_0~135Ω. The length of the branch is l_{br}=*2.55m* and has an open and short circuited notches at 19.3MHz and 38.3 MHz respectively. The analysis is performed for (a) loads with different constant impedances (b) capacitive load of different values (c) inductive loads of different values (d) constant complex loads with different real and imaginary components (e) RLC loads having different real and imaginary components. The results of the simulation for (a)-(d) are given in Figure-3 and for (e) in Figure-4. The plot of the *IA* of the branch as a function of frequency shows that: (1) the constant loads cause the branches to act as open or short circuits having minimum depth of the notches when equal to the characteristic impedance of the cable. (2) The capacitive loads (C_{br}) cause the notches to be at the short or open circuited positions for large or small ones and shifted for medium ones. (3) The inductive loads (L_{br}), cause the notches to be in the short or open circuited positions when the impedance is small or large. Medium values shift the notches from these positions. (4) Constant complex loads cause notches to be at the short or open circuited values for values that are small or large. For other values, the peaks are shifted from these positions (for e.g 2.4 MHz for 0.02-27j and 3.5 MHz for 1.5-40j). The heights of the peaks are minimized when the real part approximates the characteristic impedance of the cables. (5) The notches for RLC depend on the real, imaginary and absolute characteristics. Those having small imaginary and real characteristics cause the notches to be in the short circuited positions (RLC_1). (6) Those having non negligible imaginary characteristics shift the notches from the short circuited ones (RLC_2 and RLC_3). (7) Those having real characteristics comparable to the characteristic impedance of the cable attenuate the peaks (RLC_3).

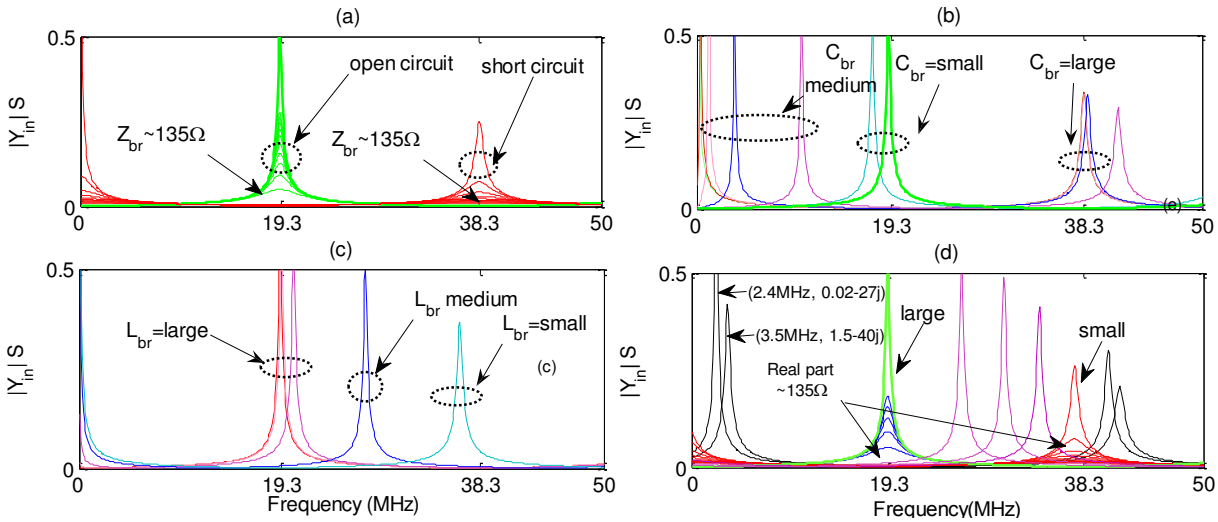

Figure-3. Admittance of the branch with (a) constant impedances of different values (b) capacitive loads of small, large and medium values (c) inductive loads with small, large and medium values (d) constant complex loads having different values.

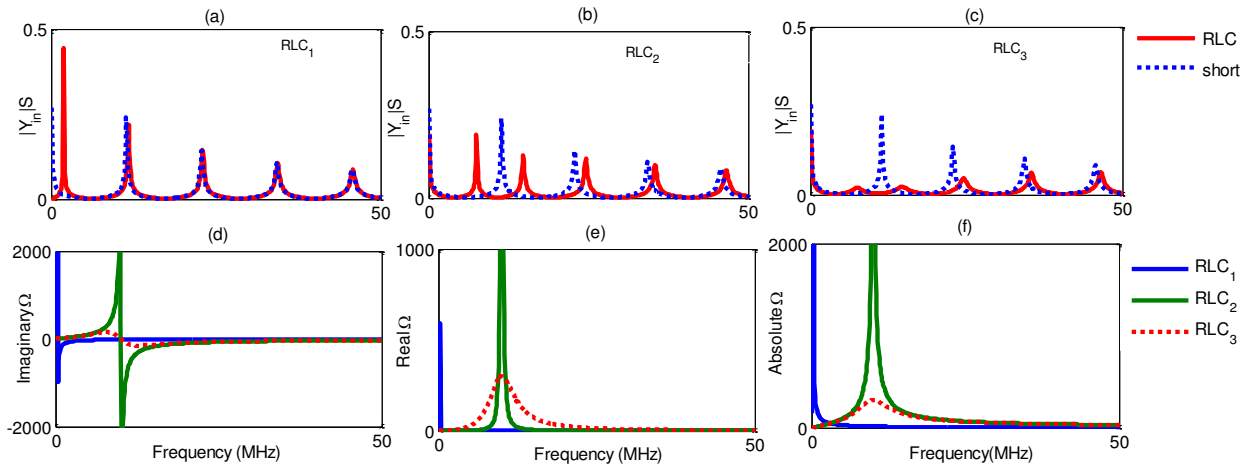

Figure-4. (a)-(c) Input admittance of the branch with RLC loads namely RLC_1, RLC_2 and RLC_3 respectively (d) imaginary components of the three loads (e) real component of the three loads (f) absolute impedance of the three loads.

As the capacitive, inductive and RLC loads like RLC_1 do not attenuate the *IA* peaks, these are expected to generate channels having low CBW for all types of cables. However loads like RLC_3 is expected to generate channels with higher value of CBW.

Experimental verification of some resoant loads

To verify the simulations, the most complex form of loads presented, namely such as RLC circuits are chosen. Simple branch with *Cable (i)* is setup and the experimental TF is evaluated for three different RLC loads in the frequency band <10MHz. The impedance of the loads is termed as (a) Z_{br1} (b) Z_{br2} and (c) Z_{br3} respectively. Figure-5(a)-(c) gives the plot of the experimental TF compared against the simulated one. In Figure-5(d)-(f), the imaginary, real and absolute characteristics of the load are plotted to analyze the TF adequately.

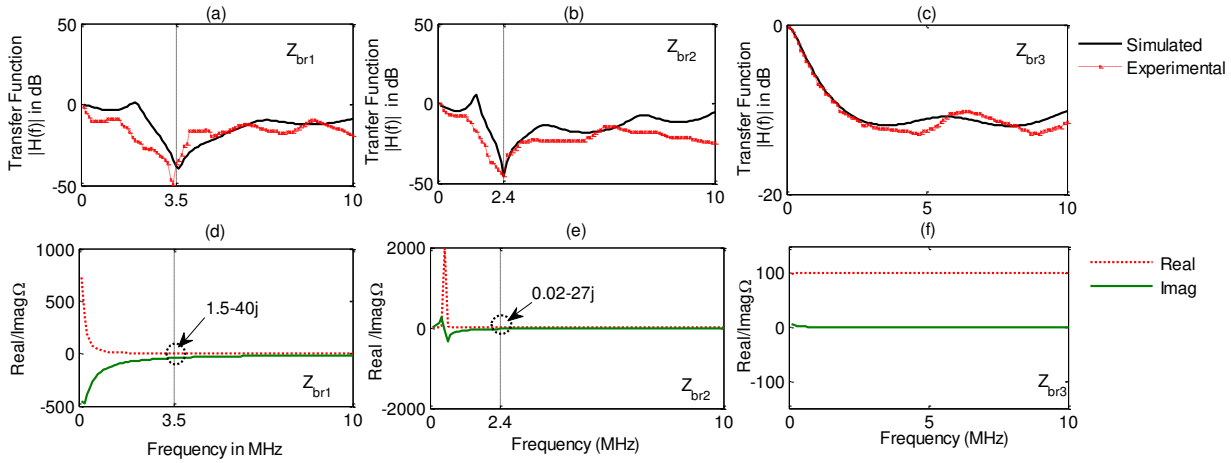

Figure-5. (a)-(c) The simulated and experimental transfer function of the three RLC loads (d)-(f) The real (real) and imaginary (Imag) characteristics of the three loads.

It is seen from the Figures that the experimental TF tallies with the simulated one. The occurrences or absence of notches is explained from the simulation of complex constant loads in Figure-3(d). For the channel with the load Z_{br1}, a notch at 3.5 MHz is found. The load at this frequency is (1.5-40j) and from Figure-3(d), it is seen that such a complex constant load at the branch also produces a notch at this frequency. Similarly, for Z_{br2} the notch at 2.4MHz occurs as the load at this frequency (0.02-27j) also produces a notch at this frequency for complex constant loads. The results show that for frequency dependent loads, notches occur when the same is also predicted for fixed loads having the same components at the particular frequency. In Z_{br3}, the absence of the notch is because the real component of the impedance is comparable to the Z_0 of the cable used.

Effect of channel variability on frequency selectivity

Coherence bandwidth, statistical variations and RMS delay spread of test conditions

To analyze the frequency selectivity of the dependencies, the CBW of channels constituted of cables with different *L* and *C* is evaluated (Table-1). The CBW is the range of frequencies over which the channel can be considered approximately flat. It is defined as the interval of frequencies at which the normalized autocorrelation function (14) of the response of the channel is higher than a certain value (usually taken as 0.9).

$$R(t,\Delta f)=\sum_{t=0}^{M} H(t,f)H(t,f+\Delta f) \tag{14}$$

Channels are constituted having branch lengths $(0m < l_{br} < 10m)$ and loads selected using a random number generator. The channel is constituted of *Cable (i)* and analysis is done up to 50MHz. The loads are from a pool of inductive, capacitive, resistive loads and RLC circuits. Different types of test channels are considered with (a) only one branch with randomly selected lengths and loads (b) 10 branches with randomly selected lengths and loads (c) *star* branches with 3/8 number of branches at the node (d) *bus* branches with 3/8 number of branches (e) 10 branches with RLC loads as RLC_1 (f) 10 branches with RLC loads such as RLC_3. For every value of *LC* and test conditions, 100 numbers of random channels are generated and the average CBW is found out. The standard deviation of the CBW and the RMS Delay Spread (RMS-DS) is also found out. The CBW directly affects the RMS-DS given by

$$\tau_{RMS}(\mu s)=\frac{55}{B_{0.9}(KHz)}$$

Figure-6 (a) shows the plot of CBW for different test channels as a function of the logarithm of *LC*. It is seen that the CBW of all the test channels constituted of cables with small *R* and *G* (*Type-1*) is larger for those with smaller *LC*. The decrease is shown as a fit in the figure. However, cables of the category *Type-2*, has a much larger CBW than the *Type-1* cables and cannot be fitted adequately. The CBW of channels loaded with RLC_3 greater than when loaded with RLC_1. This is because the real component of RLC_3 approximates the Z_0 of the cable used in the BW of observation. The improvement of the CBW in this case is so large that it approaches the condition of one loaded branch channel. Large CBW implies smaller RMS DS (Figure-6(b)) which improve the transmission rate of communication. From the plot of the σ, in Figure-6(c), it is seen that the channels with larger CBW show higher variations than smaller ones.

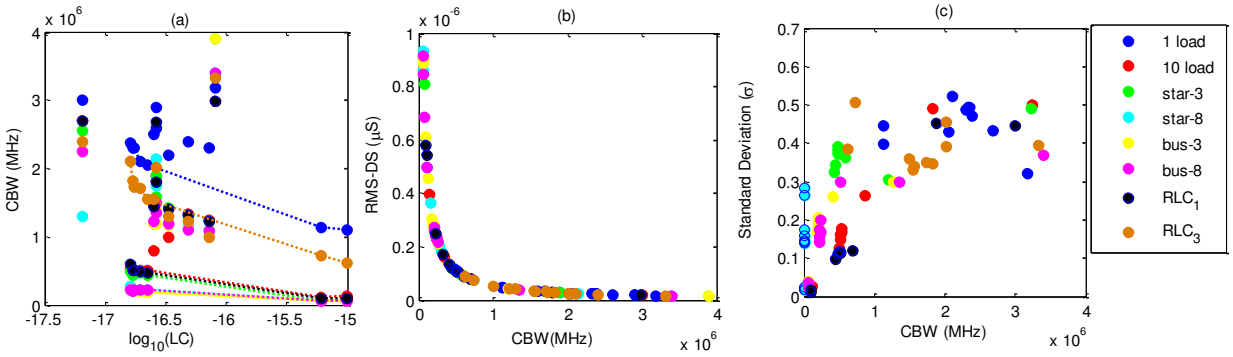

Figure-6. (a) Average coherence bandwidth of cables for different test channels. The fit shows the variation of CBW for *Type-1* cases. The data points beyond the fit are for *Type-2* cases (b)) the RMS DS as a function of the average coherence bandwidth (c) Standard deviation of 100 random channels of the test channel as a function of the average coherence bandwidth.

CONCLUSIONS

In this work, the dependence of frequency selectivity of PL channels on the network variability like cables, loads and topology is done. The available PL cables can be divided into two groups: *Type 1* and *Type-2*. *Type-1*, cables show smaller CBW than *Type -2* cables. For *Type-1* cables, the CBW decreases for increasing *LC*. It must be noted that the cable parameters are not constant, but depend on the shape and geometry of the conductors, permittivity of the insulating medium and also on the type of signal coupling used for transmission. The PL cables, therefore, can be predicted towards their efficiency as a communication channel. Out of all the loads that are connected to the PL, those having real components approximating the characteristic impedance of the cables can improve the CBW. It has been found that, most of the loads used have this time invariant frequency dependent resonant behavior. Those with short term linear periodic time variant (LPTV) nature also have similar behavior for a large fraction of time [16]. The characteristics of these loads can also be optimized beforehand. An increase in the CBW can be translated to smaller RMS-DS and faster symbol transmission rates. The deterministic study has given a broad picture of the effect of network variability on the TF of PL channels. The results can be kept in mind in the future implementation of PL networks, design of cables and modeling of loads aiming power delivery and as a communication channel.

REFERENCES

[1] Biglieri E. 2003. Coding and Modulation for a horrible channel. IEEE Communications magazine. 41(5): 92-98.

[2] Anatory J., Theethayi N., Thottappillil R., Kissaka MM. and Mvung NH. 2007. The Effects of Load Impedance, Line Length, and Branches in the BPLC-Transmission-Line Analysis for Indoor Voltage Channel. IEEE Transaction on Power Delivery. 22(4): 2150-2155.

[3] Mlynek P., Misurec J., Koutny M. 2013. Random Channel Generator for Indoor Power Line Communication. Measurement Science Review. 13(4): 206-213.

[4] Galli S., Banwell T. 2014. A deterministic frequency-domain model for the indoor power line transfer function. IEEE Journal on Selected Areas in Communications. 24(7): 1304-1316.

[5] Tlich M., Zeddam A., Moulin F., Gauthier F. 2008. Indoor Power-Line Communications Channel Characterization up to 100 MHz-Part II: Time-Frequency Analysis. IEEE Transactions on Power Delivery. 23(3): 1402-1409.

[6] Marrocco G., Statovci D. 2013. A PLC Broadband Channel Simulator for Indoor Communications. International Symposium of Power Line Communications and Applications. pp. 321-326.

[7] Tan B. Thomson J. 2012. Parameter Appendix. [Online] Available: http://www.arxiv.org/pdf/1203.3245.pdf.

[8] Hossain E., Khan S., Ali A. 2008. Modeling Low Voltage Power Line as a Data Communication Channel. International Journal of Electric Computer Energetic Electronics and Communication Engineering. 2(9): 76-80.

[9] Ahola J. Application of Power Line Communication to Data Transfer of On-line Condition Monitoring of Electrical Drives. Ph.D https://www.doria.fi/bitstream/handle/10024/31175/TMP.objres.311.pdf, Date assessed: 4th May 2015.

[10] Khan S., Salami AF., Lawal WA., Alam AHMZ., Hameed SA., Salami MJE. 2008. Characterization of Indoor Power lines As Data Communication Channels Experimental Details and Results. Engineering and Technology. 2(10): 519-524.

[11] Tsuzuki S., Yamamoto S., Takamatsu, T. 2001. Measurement of japanese indoor power-line channel. 5th International Symposium on Power-Line Communication and Its Applications (ISPLC). pp. 79-84.

[12] Tiru B., 2015. Characteristics of Transfer Function of Power Lines having Tapped Branches in the Propagation Path. International Conference on Computing, Communication and Security (ICCCS). pp. 1-7.

[13] Canete F., Cortes J., Dies L., *et al*. 2011. A channel model proposal for indoor power line communications. IEEE Communications Magazine. 49(12): 166-174.

[14] Esmailian T., Kschischang K R., Gulak P G. 2003. In-building power lines as high-speed communication channels: channel characterization and a test channel ensemble. International Journal of Communication System. 16: 381-400.

[15] Tonello A., Versolatto F., Pittolo A. 2014. In-Home Power Line Communication Channel: Statistical Characterization. IEEE Transactions on Communications. 62(6): 2096-2106.

[16] Corripio FJC., Arrabal JAC., Río LD., Muñoz JTE. 2006. Analysis of Cyclic Short Term Variation of Power Line Channels. IEEE Journal on Selected Areas on Communication. 24(7): 1327-1338.